MOLECULAR AND CELLULAR BIOLOGY, Apr. 2005, p. 3127–3139 Vol. 25, No. 8
0270-7306/05/$08.00+0 doi:10.1128/MCB.25.8.3127–3139.2005

RAD-51-Dependent and -Independent Roles of a *Caenorhabditis elegans* BRCA2-Related Protein during DNA Double-Strand Break Repair†‡

Julie S. Martin, Nicole Winkelmann, Mark I. R. Petalcorin, Michael J. McIlwraith, and Simon J. Boulton*

Clare Hall Laboratories, London Research Institute, Cancer Research UK, South Mimms, Hertfordshire, United Kingdom

Received 26 November 2004/Returned for modification 27 December 2004/Accepted 24 January 2005

The BRCA2 tumor suppressor is implicated in DNA double-strand break (DSB) repair by homologous recombination (HR), where it regulates the RAD51 recombinase. We describe a BRCA2-related protein of *Caenorhabditis elegans* (CeBRC-2) that interacts directly with RAD-51 via a single BRC motif and that binds preferentially to single-stranded DNA through an oligonucleotide-oligosaccharide binding fold. *Cebrc-2* mutants fail to repair meiotic or radiation-induced DSBs by HR due to inefficient RAD-51 nuclear localization and a failure to target RAD-51 to sites of DSBs. Genetic and cytological comparisons of *Cebrc-2* and *rad-51* mutants revealed fundamental phenotypic differences that suggest a role for *Cebrc-2* in promoting the use of an alternative repair pathway in the absence of *rad-51* and independent of nonhomologous end joining (NHEJ). Unlike *rad-51* mutants, *Cebrc-2* mutants also accumulate RPA-1 at DSBs, and abnormal chromosome aggregates that arise during the meiotic prophase can be rescued by blocking the NHEJ pathway. CeBRC-2 also forms foci in response to DNA damage and can do so independently of *rad-51*. Thus, CeBRC-2 not only regulates RAD-51 during HR but can also function independently of *rad-51* in DSB repair processes.

[1]The faithful segregation of homologous chromosomes during meiosis is dependent on the formation of physical connections (chiasmata) that form following the successful reciprocal exchange of DNA molecules resulting from crossover recombination. In concert with sister chromatid cohesion, chiasmata facilitate the proper orientation of homologous chromosomes and their subsequent segregation to opposite poles of the meiotic spindle (53). In most eukaryotes, meiotic recombination is initiated by the action of Spo11, a topoisomerase II-like enzyme that catalyzes the formation of meiosis-specific DNA double-strand breaks (DSBs) (15, 18). Once formed, a DSB is processed to generate a resected 3′ single-stranded DNA (ssDNA) tail that is rapidly bound by replication protein A (RPA) before being displaced by RAD51, the eukaryotic homolog of the bacterial DNA strand exchange protein RecA. Rad51 catalyzes DNA strand exchange between homologous sequences, thus promoting the physical exchange of DNA molecules required for successful crossover recombination.

Many of the genes required for meiotic recombination also function in the repair of DSBs generated following exposure to DNA-damaging agents or arising following the collapse of stalled replication forks. The importance of these genes in preventing genome instability is highlighted by the plethora of human cancer susceptibility syndromes that arise from defects in DNA repair genes (20). For example, inherited mutations in the DNA repair gene *BRCA2* lead to an enhanced predisposition to breast, ovarian, and other cancers (37). Defects in *BRCA2* are also responsible for the D1 complementation group of Fanconi anemia, an autosomal recessive disorder characterized by cancer predisposition, congenital defects, progressive bone marrow failure, and hypersensitivity to DNA cross-linking agents, such as cisplatin and mitomycin C (16). It is widely accepted that BRCA2 functions in the homologous recombination (HR) pathway—an error-free mechanism of DSB repair (DSBR) that utilizes an intact sister or homologous chromosome to repair breaks in DNA (19, 45). In the absence of HR, gross chromosomal rearrangements, such as deletions and translocations, result from error-prone repair of spontaneous DSBs (17). Such gross chromosomal rearrangements are the hallmark of *BRCA2*-defective cells (44, 51).

Accumulating evidence supports a direct role for BRCA2 in HR, where it functions as a regulator of RAD51 (46). First, BRCA2 and RAD51 proteins colocalize extensively at sites of DSBs, suggesting that they may form a complex in vivo (10). The 3,418-amino-acid human BRCA2 protein binds directly to RAD51 through a BRC motif that is repeated eight times within the central region of the protein (11, 49). Overexpression of the BRC4 motif in cell cultures confers a dominant-negative radiation-sensitive phenotype and an inability to form RAD51 foci at gamma irradiation-induced DSBs (9). Similarly, mutant cell lines harboring truncations in *BRCA2* are radiation sensitive, fail to form RAD51 foci at DSBs, and are severely compromised in the homology-directed repair of DSBs (29, 32, 52). Finally, peptides corresponding to the BRC3 or BRC4 motif also block RAD-51 multimerization, forcing it into a monomeric state that is unable to bind DNA or perform recombination reactions in vitro (14). Together with the obser-

* Corresponding author. Mailing address: Clare Hall Laboratories, London Research Institute, Cancer Research UK, Blanche Ln., South Mimms, Hertfordshire EN6 3LD, United Kingdom. Phone: 44 1707 625774. Fax: 44 208 269 3801. E-mail: simon.boulton@cancer.org.uk.

† Supplemental material for this article may be found at http://mcb.asm.org/.

‡ We dedicate this work to the memory of Nicole Winkelmann.

vation that RAD51 is predominantly cytoplasmic in the absence of BRCA2, it has been speculated that BRCA2 imposes two levels of control over RAD51 function by regulating its cellular localization and modulating its repair activities (19, 46). However, the mechanism by which this control occurs and whether BRCA2 performs a similar role in meiotic recombination are not known.

Five distinct structural domains have been identified in the cocrystal structure of the C-terminal region of BRCA2 bound to DSS1, a highly conserved 70-amino-acid acidic protein shown previously to bind to BRCA2 (30, 50). These include a helical region, three oligonucleotide-oligosaccharide binding (OB) folds that are also present in ssDNA binding proteins such as RPA, and a tower-like extension from OB fold 2 that may bind to double-stranded DNA (dsDNA). A simplified version of BRCA2 has been identified in the fungus *Ustilago maydis* (Brh2); it possesses a single BRC motif and a C-terminal conserved region containing two OB folds, including the tower-like extension found in OB fold 2 of the human protein (21). Brh2 and the single Dss1 homolog in *U. maydis* function in the Rad51 pathway for HR, as their combined disruption results in epistatic DNA repair and meiotic recombination defects (22). Meiotic defects also arise in the absence of *Arabidopsis thaliana* BRCA2, adding further support to a conserved role for BRCA2 orthologs in meiotic recombination (41). At present, very little is known about the role of BRCA2 in meiotic recombination other than that it plays a role in the Rad51 pathway.

The work presented here describes the identification of a BRCA2-related protein of *Caenorhabditis elegans* (CeBRC-2). Although CeBRC-2 is only a little over a tenth the size of its human counterpart, it possesses a single BRC domain, an OB fold, and two putative nuclear localization signals (NLSs) that are hallmarks of BRCA2 proteins (25). We propose that CeBRC-2 is functionally related to BRCA2 in human cells based on the observations that CeBRC-2 binds directly to RAD-51 and ssDNA and that *Cebrc-2* mutants fail to repair meiotic and radiation-induced DSBs by HR due to an inability to correctly regulate RAD-51. Importantly, these studies also reveal fundamental differences between *Cebrc-2* and *rad-51* mutants that may indicate previously unknown functions for BRCA2-related genes in DNA repair.

MATERIALS AND METHODS

Worm strains. *C. elegans* strains were cultured as described previously (7). The following strains were kindly provided by the *Caenorhabditis* Genetics Center (University of Minnesota, St. Paul): wild-type Bristol N2, *spo-11* (*ok79*), *rad-5* (*mn159*), and *rad-51* (*Ig08701*) (1, 2, 15). The *brc-2* (*tm1086*) and *lig-4* (*ok716*) deletions were isolated by the National Bioresource Project for the Nematode, Department of Physiology, School of Medicine, Tokyo Women's Medical University, Tokyo, Japan, and the *C. elegans* Knockout Consortium, respectively. Deletions were outcrossed six times with the wild-type Bristol N2 strain and then balanced with JK2739 [*lin-6* (*e1466*) *dyp-5* (*e61*) *I*/*nT2* (*qIs48*) (*I*,*II*)]. RNA interference (RNAi) depletion of *lig-4* was performed by the RNAi feeding method as previously described (5).

Sequence alignments. Protein sequences were aligned by using Pileup and refined by using the Lineup algorithm (Genetics Computer Group). Multiple sequence files were exported to ESPript 2.0 at http://prodes.toulouse.inra.fr/ESPript/cgi-bin/nph-ESPript_exe.cgi for box-shading analysis.

Gateway recombinational cloning. Open reading frame-specific primers compatible with the Gateway system (Invitrogen) were designed for *Cebrc-2* and cloned into Entry as previously described (47). The sequences of primers used for *Cebrc-2* cDNA amplification can be found at http://worfdb.dfci.harvard.edu/search.pl?form=1&search=T07E3.5. Gateway LR destination cloning was used to transfer *Cebrc-2* cDNA into pAD-Amp and pDB-Amp (for yeast two-hybrid analysis), pDEST-CMV-Flag and pDEST-CMV-Myc (for protein expression in 293T cells), and pSB_GW::TAG (for generating integrated transgenic lines).

Protein interaction assays. The yeast two-hybrid methods used were previously described (5). To test pair-wise interactions in yeast cells, Gal4 DNA binding domain and activation domain fusions were used to cotransform yeast strain MAV103. Interactions for each combination were tested by scoring for yeast two-hybrid phenotypes (LacZ and Ura) at 30°C as described previously (5).

To test for interactions directly with recombinant proteins, BL21(DE3) codon plus bacterial strains were transformed with pET22_*rad-51*, pET28_*brc-2*-6His, and/or pET28_*brc-2*. Protein expression was induced for 3 h at 30°C with 0.5 mM isopropyl-β-D-thiogalactopyranoside (IPTG). Cells were harvested, lysed in TLB (50 mM sodium phosphate [pH 7.0], 20 mM imidazole, 250 mM NaCl, 10% glycerol, protease inhibitor cocktail [Invitrogen]), and treated with 5 μg of DNase I (Sigma)/ml prior to clarification of extracts at 42,000 × *g* in a Beckman ultracentrifuge for 30 min. Extracts were incubated with preequilibrated Talon beads for 30 min at 4°C before being washed three times with TLB. Proteins associated with the beads were subjected to 10% polyacrylamide gel electrophoresis (PAGE) and then visualized by Coomassie brilliant blue staining.

To test for interactions in tissue culture cells, 293T cells were transiently transfected with pDEST-CMV_Flag-*brc-2*, pDEST-CMV_Myc-*rad-51*, or pDEST-CMV_Myc constructs by using Lipofectamine 2000 (Gibco BRL). At 72 h posttransfection, cells were harvested, lysed in ELB250 (50 mM HEPES [pH 7.0], 250 mM NaCl, 0.5% NP-40, 0.5 mM EDTA, 1 mM phenylmethylsulfonyl fluoride, 0.5 mM NaF, 0.1 mM Na_2VO_3, 0.5 mM dithiothreitol [DTT], protease inhibitor cocktail), and treated with 5 μg of DNase I/ml prior to clarification of extracts at 42,000 × *g* in a Beckman ultracentrifuge for 30 min. Extracts were incubated with monoclonal antibody (MAb) 9E10 (Myc) or M2 (Flag) coupled to beads for 30 min at 4°C before being washed three times with ELB250. Proteins associated with the beads were subjected to electrophoresis and then Western blotting with MAb 9E10 (Myc) or M2 (Flag) as previously described (6).

To test for an interaction between CeBRC-2 and RAD-51 by coimmunoprecipitation from *C. elegans* extracts, the pSB_$P_{brc\text{-}2}$*brc-2*::HA_8×His_TEV_Myc transgene was delivered into *unc-119* (*ed3*) by microparticle bombardment, and the *dwIs7*-transformed line was selected as previously described (36). Extracts prepared from N2 (wild-type) and *dwIs7 C. elegans* strains were incubated with MAb 9E10 (Myc) or 12CA5 (hemagglutinin [HA]) coupled to beads for 30 min at 4°C before being washed three times with lysis buffer as previously described (35). Proteins associated with the beads were subjected to electrophoresis and then Western blotting with antibody to BRC-2 or RAD-51.

CeBRC-2 protein purification. BL21(DE3) codon plus bacteria were transformed with pET28_*brc-2*-6His and used to inoculate 20 liters of fermenter broth (32 g of Bacto tryptone/liter, 20 g of Bacto yeast extract/liter, 5 g of NaCl/liter, 10 g of K_2HPO_4/liter, 1.85 g of KH_2PO_4/liter, 50 μg of kanamycin/ml, 25 μg of chloramphenicol/ml) in a 40-liter BioFlow500 fermenter (New Brunswick). Protein expression was induced with 1 mM IPTG at 16°C overnight. Cells were harvested, and 10 g of cell pellet was resuspended in lysis buffer (50 mM NaP [pH 7.0], 500 mM NaCl, 10% glycerol) and lysed with a French press. Extracts were incubated with 2 μg of DNase I/ml for 1 h before centrifugation. CeBRC-2(His_6) was purified by ammonium sulfate precipitation (final concentration, 66%), Talon affinity chromatography (elution with a 50 to 500 mM imidazole gradient), and heparin chromatography. Peak CeBRC-2(His_6) fractions were pooled and dialyzed against protein storage buffer (20 mM Tris-acetate [pH 7.5], 200 mM potassium acetate, 10% glycerol, 1 mM EDTA, 0.5 mM DTT). Purified CeBRC-2(His_6) is devoid of nuclease contamination and, following sodium dodecyl sulfate (SDS)-PAGE, is the only protein detected by silver staining.

DNA binding assays. Binding reaction mixtures (10 μl) contained 5′-^{32}P-end-labeled DNA substrates (0.5 ng or 0.15 nM) and various amounts of CeBRC-2 in binding buffer (50 mM Tris-HCl [pH 8.0], 5 mM EDTA, 1 mM DTT, 100 μg of bovine serum albumin/ml, 6% glycerol). After 10 min of incubation at room temperature, products were analyzed by 4% PAGE with Tris-borate-EDTA buffer and visualized by autoradiography. The 5′-^{32}P-end-labeled 100-mer and complementary oligonucleotides were prepared as described previously (31). Samples (see Fig. 2F; see also Fig. S1A in the supplemental material) were resolved for 1 h and for 3 h at 100 V, respectively; it was necessary to resolve some of the protein-DNA complexes (see Fig. S1A in the supplemental material) for a longer time in order to observe the supershifted complexes with the His antibody.

Generation of transgenic lines. A 3.545-kb PCR product that includes the entire coding and promoter region of the T07E3.5 gene (see Results) was amplified from T07E3 cosmid DNA with primers having the sequences GGGG ACAAGTTTGTACAAAAAAGCAGGCTTGCCTATTTTCGTTTTCCAAAG

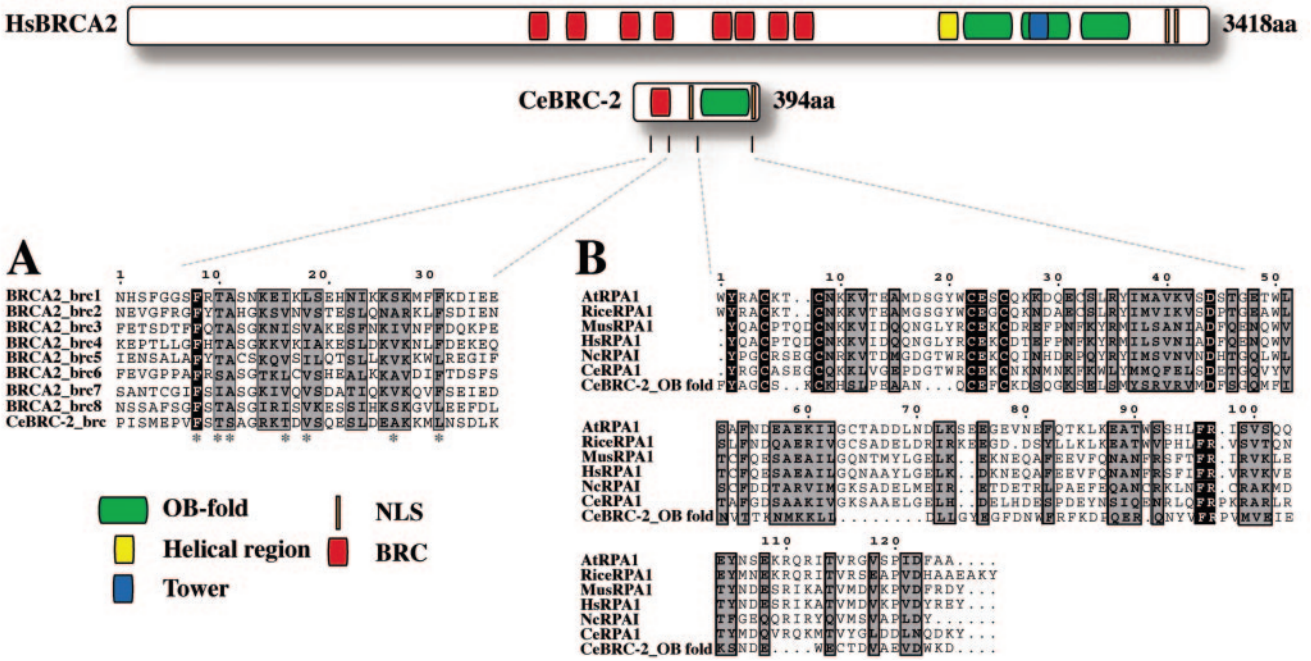

FIG. 1. CeBRC-2 possesses a subset of conserved domains present in human BRCA2. A scaled representation of human BRCA2 compared with CeBRC-2 is shown at the top. The various conserved domains, including the BRC repeat region (red), the helical region (yellow), OB folds (green), the tower-like structure (blue), and putative NLSs (black-orange), are indicated. The single BRC motif (residues 9 to 114) in CeBRC-2 is situated at the N terminus of CeBRC-2. Two putative NLSs are located on either side of a single OB fold situated at the C terminus of the protein (residues 263 to 370). aa, amino acids. (A) Protein sequence alignment of the eight BRC motifs of BRCA2 (abbreviated brc1 to brc8) with the single BRC motif of CeBRC-2 (CeBRC-2_brc). Asterisks indicate the critical residues required for the BRC4-Rad51 interaction, as defined structurally (34). (B) Alignment of the OB fold domain of CeBRC-2 (CeBRC-2_OB fold) with the OB fold of RPA1 from six different species (At, *A. thaliana*; rice; Mus, mouse; Hs, human; Nc, *Neurospora crassa*; and Ce, *C. elegans*).

TCTCG and GGGGACCACTTTGTACAAGAAAGCTGGGTATGGATGCT TCTTTTTCGAACGG. The PCR product was cloned by Gateway recombination into p221 Entry and subsequently into pSB_GW::tag to generate pSB_$P_{brc\text{-}2}$*brc-2*::*Tag* as previously described (35). The *dwIs7* ($P_{brd\text{-}1}$*brd-1*::*tag*) transgenic line then was generated by microparticle bombardment of *unc-119* (*ed3*) animals with pSB_$P_{brc\text{-}2}$*brc-2*::*Tag*. The $P_{brd\text{-}1}$*brd-1*::*tag* transgene appears to retain biological function, as it is able to rescue the embryonic lethality of *brc-1* (*tm1086*) mutants (data not shown).

Peptide synthesis and production of antibodies. Peptides were synthesized (Peptide Synthesis Laboratory, Cancer Research UK) for antibody production (BRC-2N, N-CMGDSSKKVKDSFDTISEPD-C; BRC-2C, N-CWKDFGSYL KHKEDKKKRRS-C) and for microinjection (BRC_Wt, N-CDEPKGVPISM EPVFSTAAGIRIDVKQESIDKSKKMLNSDLKSKSSSKGGFSSPLVRKNNG SSAFVSPF-C; BRC_Mut, N-CDEPKGVPISMEPVFIDVKQESIDKSKKM LNSDLKSKSSSKGGFSSPLVRKNNGSSAFVSPF-C). For antibody production, 1 mg each of BRC-2N and BRC-2C peptides was coupled to activated keyhole limpet hemocyanin (Pierce, Rockford, Ill.) before injection into rabbits (Harlan Sera Labs, Loughborough, United Kingdom). Affinity purification of antibodies was performed by binding reacting antibodies from the crude serum to an immobilized peptide-Sulfolink matrix (Pierce). The column was washed extensively with coupling buffer prior to elution with Gentle Ag/Ab elution buffer (Pierce). Eluted antibodies were dialyzed against protein dilution buffer (20 mM Tris-HCl [pH 7.8], 200 mM potassium acetate, 10% glycerol, 1 mM EDTA, 0.5 mM DTT). Antibodies were tested by Western blotting against recombinant proteins expressed in *Escherichia coli* and then against *C. elegans* extracts. Extracts were generated from a pellet of frozen mixed-staged wild-type Bristol N2 worms by lysis in buffer A {7 M urea, 2 M thiourea, 4% 3-[(3-cholamidopropyl)-dimethylammonio]-1-propanesulfonate (CHAPS), 40 mM Tris, 65 mM DTT}.

Cytological preparation and immunostaining. Gravid hermaphrodites were transferred to 30 μl of phosphate-buffered saline (PBS) on poly-L-lysine-coated slides (slides were washed with 70% ethanol and then given two coats of 100% poly-L-lysine, with air drying between the coats). The worms were washed with PBS before being transferred to 50 μl of 10 mM levamisole. Germ lines were extruded by removing the head and tail with a fine-gauge (27-gauge) needle. Levamisole was replaced with 1% paraformaldehyde in PBS for 10 min. After fixation, the germ lines were permeabilized for 5 min in TBSB (Tris-buffered saline–0.5% bovine serum albumin)–0.1% Triton X-100 and washed with TBSB at least three times for 5 min each time, followed by blocking for 30 min. Primary antibodies were diluted in TBSB (1:500 for RPA-1, 1:100 for RAD-51, 1:50 for SYP-1, and 1:2,000 for CeBRC-2 antibodies) and incubated overnight at 4°C in a humid chamber. Germ lines were subsequently washed at least three times for 5 min each time with TBSB before incubation with secondary antibodies for 1 to 2 h at room temperature (antibodies to rabbit Cy3 at 1:10,000 or to guinea pig-fluorescein isothiocyanate at 1:10,000 [Sigma]). Finally, the germ lines were washed at least three times for 5 min each time with TBSB (second wash also containing 1 μg of 4′,6′-diamidino-2-phenylindole [DAPI]/ml) before being mounted on coverslips with Vectashield.

Fluorescence microscopy. Deltavision microscopy was used to examine germ lines with either a ×40 or a ×63, 1.4 NA Planapochromat lens on an Olympus inverted microscope (IX71). Images were captured by using SoftWorx computer software (Applied Precision). Three-dimensional data sets were computationally deconvolved, and regions of interest were projected onto one dimension. Merged or single-color images were recorded by using GIMP software.

RESULTS

Identification of CeBRC-2 through its association with RAD-51. From a yeast two-hybrid screen for RAD-51-interacting partners, we isolated a previously uncharacterized protein encoded by *C. elegans* gene T07E3.5. This open reading frame is predicted to encode a 394-amino-acid protein (Fig. 1). PSI-BLAST sequence homology searches of the N-terminal 114 amino acids of the protein revealed a single BRC domain, a RAD51 binding motif that is present in variable copy numbers in BRCA2 orthologs: human (eight BRCs), *U. maydis* (one

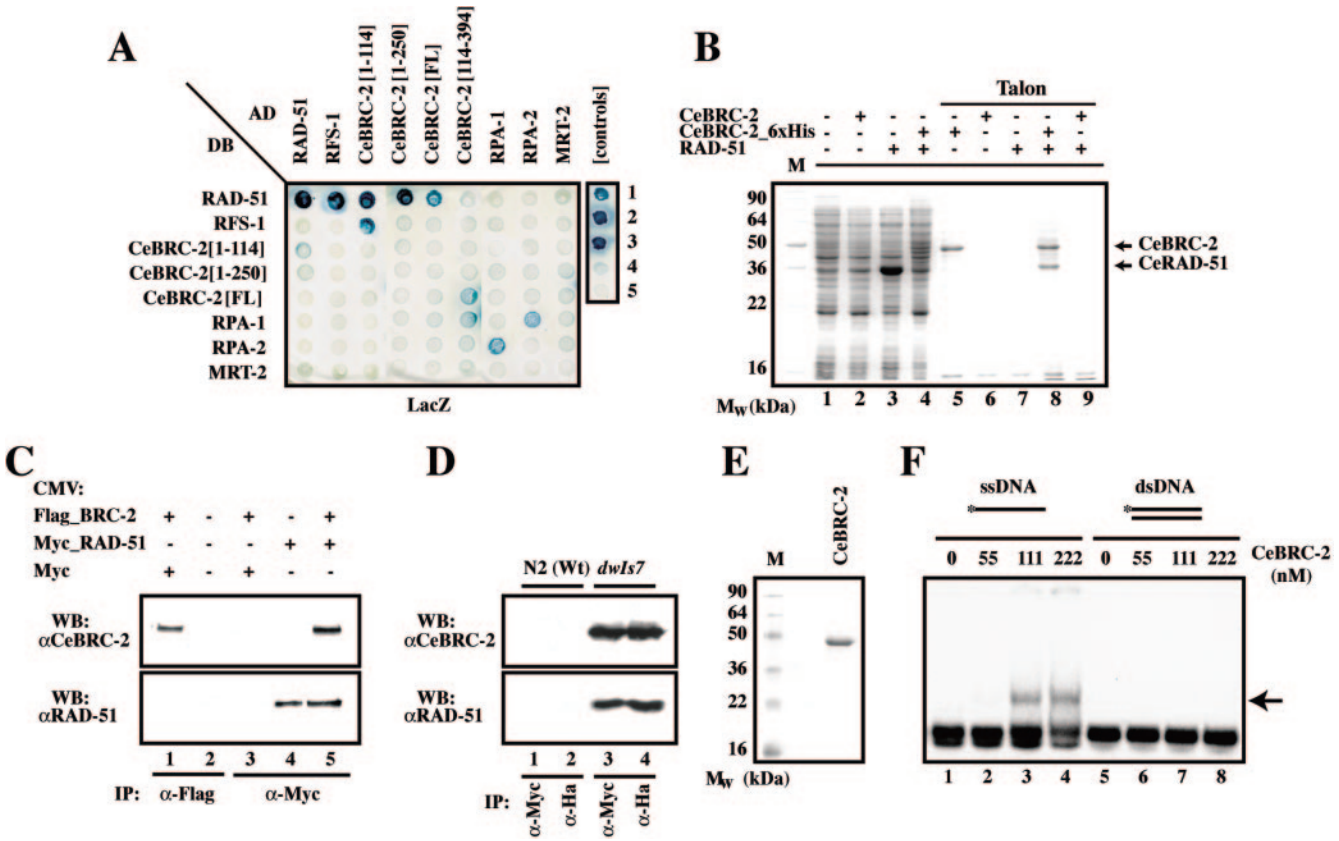

FIG. 2. CeBRC-2 and RAD-51 interact directly in vitro and in vivo. (A) The yeast two-hybrid system was used to test for protein interactions among RAD-51, RAD-51D, CeBRC-2 (residues 1 to 114), CeBRC-2 (1 to 250), CeBRC-2 (full length [FL]), CeBRC-2 (114 to 394), RPA-1, RPA-2, and MRT-2 fused to either the DNA binding domain (DB) or the activation domain (AD) of GAL4 by scoring for *lacZ* expression. Controls: 1, DB-DP and AD-E2F1; 2, Gal4p and AD; 3, DB-Fos and AD-Jun; 4, DB-pRB and AD-E2F1; and 5, DB and AD without any fusion (5). Lane M, markers. (B) CeBRC-2, CeBRC-2(His_6), and RAD-51 were expressed in *E. coli* (10% of the whole-cell extracts used in the pull-down assays is shown in lanes 1 to 4), and pull-down assays were performed with whole-cell extracts and Talon beads, which specifically bind to proteins containing polyhistidine tracks. RAD-51 was pulled down on Talon beads with full-length C-terminal histidine-tagged Ce-BRC-2 (lane 8) but not when expressed alone (lane 7) or with untagged CeBRC-2 (lane 9). Pull-down assay samples were resolved by SDS–12% PAGE and stained with Coomassie brilliant blue. (C) Flag-tagged CeBRC-2 was coimmunoprecipitated with anti-Myc MAb 9E10 when coexpressed in 293T cells with CMV_Myc-RAD-51 (lane 5) but not with CMV_Myc (lane 3). WB, Western blot; IP, immunoprecipitation. Approximately 30% of Myc-RAD-51 in the extracts was pulled down with Flag-tagged CeBRC-2. (D) Ce-BRC-2 and RAD-51 were coimmunoprecipitated with anti-Myc MAb 9E10 (lane 3) and anti-HA MAb 12CA5 (lane 4) from extracts derived from the *C. elegans dwIs7* ($P_{brc\text{-}2}$*brc-2*::HA_8×His_Tev_Myc) transgenic line, which expresses CeBRC-2 fused at the C terminus to HA_8×His_Tev_Myc epitopes, but not from extracts derived from an untagged strain (lanes 1 and 2). Wt, wild type. We estimated that 30 to 35% of the RAD-51 pool in the extracts was pulled down with CeBRC-2. (E) Purified full-length recombinant CeBRC-2(His_6). An SDS–12% PAGE analysis of purified CeBRC-2(His_6) stained with Coomassie brilliant blue is shown. (F) DNA binding activity of CeBRC-2. DNA binding reactions with mixtures containing ssDNA or dsDNA and the indicated concentrations of CeBRC-2 were carried out as described in Materials and Methods. Protein-DNA complexes (indicated by an arrow) were analyzed by 4% PAGE. Asterisks indicate 5′-^{32}P-end labels.

BRC), and *A. thaliana* (four BRCs) (11, 21, 41, 49). Pair-wise alignment of the single BRC of T07E3.5 with the eight BRC motifs (brc1 to brc8) of human BRCA2 revealed that the residues required for the BRC-Rad51 interaction, identified in the BRC4-Rad51 cocrystal structure, are conserved (Fig. 1A) (34).

Sequence analysis of the C-terminal region of T07E3.5 identified a single OB fold domain and two putative NLSs that flank the OB fold (Fig. 1). Although the OB folds of BRCA2 and T07E3.5 appear to be unrelated to each other in sequence, the three OB folds of BRCA2 are structurally related to the ssDNA binding domain of RPA (50). In turn, RPA has extensive sequence similarity to the OB fold of T07E3.5, as shown by the alignment of OB folds of RPAs of various species with the OB-fold domain in T07E3.5 (Fig. 1B). Although there is an ortholog of DSS1 in *C. elegans* (Y119D3B.15), with greater than 75% sequence identity to its human counterpart, the helical region-OB fold 1 region that binds DSS1 in human BRCA2 is not obviously conserved in CeBRC-2. It therefore remains to be seen whether CeDSS-1 and CeBRC-2 interact and function together in DSBR processes.

The presence of a single BRC motif, two NLSs, and an OB fold suggests that T07E3.5 may encode an ancestral BRCA2-related protein in *C. elegans*. We therefore refer to T07E3.5 as *Cebrc-2*.

RAD-51 interacts directly with CeBRC-2 in vitro and in vivo. To determine whether the BRC motif in CeBRC-2 is responsible for the association with RAD-51, we tested various regions of CeBRC-2 for interactions with RAD-51 by using the yeast-two hybrid system. Fragments of CeBRC-2 containing

the BRC motif (amino acids 1 to 114) interact with RAD-51, as demonstrated by β-galactosidase activity (Fig. 2A). The CeBRC-2 fragment containing amino acids 1 to 114 is also capable of interacting with the single *C. elegans* RAD51 paralog (RFS-1), but the relevance of this interaction is presently unclear. However, RPA-1, RPA-2, MRT-2, and a C-terminal fragment of CeBRC-2 (amino acids 114 to 394) with a deletion of the BRC motif do not interact with RAD-51. This result demonstrates that the BRC region of CeBRC-2 is responsible for binding to RAD-51. Thus, CeBRC-2 and RAD-51 interact in a manner similar to that reported for BRCA2 and RAD51 in human cells and BRCA2 and DMC1 in *A. thaliana* (11, 41). We also tested for a previously reported association between MRT-2 and CeBRC-2 (23) but were unable to detect this interaction in either orientation in the yeast two-hybrid system (Fig. 2A).

To determine whether the CeBRC-2–RAD-51 interaction is direct, we tested for an association between CeBRC-2 and RAD-51 coexpressed in either *E. coli* or tissue culture cells. Six-histidine-tagged CeBRC-2 pulls down RAD-51 from *E. coli* extracts (Fig. 2B; see Materials and Methods). Furthermore, Myc-tagged RAD-51 is coimmunoprecipitated with CeBRC-2 from 293T cell extracts by antibodies to the Myc epitope (Fig. 2C). Since the extracts derived from both *E. coli* and 293T cells coexpressing CeBRC-2 and RAD-51 were extensively treated with DNase I to remove DNA, the CeBRC-2–RAD-51 interaction is likely to be direct and to not require DNA.

To test whether this interaction occurs in vivo, we generated *dwIs7*, a transgenic *C. elegans* line that carries a single integrated copy of a $P_{Cebrc\text{-}2}$*Cebrc-2*::HA_8×His_Tev_Myc transgene, as detected by Southern blotting, and that expresses CeBRC-2 fused to HA, eight His, and Myc epitopes under the control of its own promoter. Using antibodies to either the HA or the Myc epitope fused to CeBRC-2, we could coimmunoprecipitate RAD-51 with CeBRC-2 from extracts derived from the *dwIs7* line but not from extracts made from the wild-type strain lacking the transgene (Fig. 2D). We conclude that RAD-51 and CeBRC-2 interact in vivo.

CeBRC-2 binds preferentially to ssDNA. To assess whether CeBRC-2 can bind to DNA and whether it has a preferred substrate in vitro, we used electrophoretic mobility shift assays. In these experiments, ^{32}P-end-labeled ssDNA and dsDNA molecules were used as substrates for CeBRC-2 binding. Purified full-length recombinant CeBRC-2 (Fig. 2E) preferentially forms discrete protein-DNA complexes with ssDNA templates (Fig. 2F, lanes 1 to 4) but not with dsDNA templates (Fig. 2F, lanes 5 to 8) at equivalent concentrations of CeBRC-2. While protein-DNA complexes are readily detected between ssDNA and CeBRC-2 (111 nM), the detection of complexes with dsDNA required 20-fold-higher concentrations of CeBRC-2 (2,200 nM) (data not shown). Prebinding of CeBRC-2 with an antibody to the OB fold domain at the C terminus blocks the binding of CeBRC-2 to ssDNA, whereas an antibody that recognizes the His tag fused to the N terminus of CeBRC-2 supershifts the protein-DNA complexes (see Fig. S1A in the supplemental material). These results suggest that CeBRC-2 preferentially binds to ssDNA via its OB fold domain.

Embryonic lethality and meiotic recombination defects in *Cebrc-2* mutants. Truncating mutations in mammalian BRCA2 lead to spontaneous chromosomal rearrangements and radiosensitivity due to an inability to repair DSBs correctly via the HR pathway (44, 51). Consistent with a conserved function for BRCA2-related genes in DSBR processes, deletion of *U. maydis Brh2* or *A. thaliana Brca2* results in meiotic recombination defects similar to those seen with *Rad51* mutants (21, 41). To determine whether *Cebrc-2* is required for DSBR and/or meiotic recombination, we isolated *brc-2* (*tm1086*), a deletion that completely removes exons 5 to 7 and partially deletes exon 8 (Fig. 3A and B). Although the first four exons are intact in *brc-2* (*tm1086*), Western blotting with a CeBRC-2 antibody raised against the N terminus of the protein failed to detect a truncated product of 138 amino acids that is predicted from the *brc-2* (*tm1086*) deletion (Fig. 3C). Since no CeBRC-2 product could be detected in the mutant, we believe that the *brc-2* (*tm1086*) deletion constitutes a null mutation. Consistent with an essential role in meiosis, *Cebrc-2* mutants are egg laying defective (Egl) and fail to give rise to any viable progeny due to embryonic lethality (Emb) (Fig. 4A; see also Fig. S1B in the supplemental material). The cause of the Egl phenotype is not known, but a similar phenotype occurs following gamma irradiation of animals depleted of *rad-51* by RNAi (38).

To determine whether the Emb phenotype is caused by a defect during meiosis, we analyzed *Cebrc-2* mutants for cytological defects during meiotic prophase. The *C. elegans* germ line is spatially polarized in a distal-to-proximal manner with respect to proliferation and progression through meiotic prophase. The distal end of the germ line comprises a stem cell compartment of mitotically proliferating nuclei that are followed, more proximally, by cells in progressive stages of meiosis I. Following the premeiotic S phase, nuclei enter the leptotene stage of meiosis I, during which pairs of homologous chromosomes undergo large-scale morphological reorganization in order to align along their lengths. Aligned homologs "zip" together (synapsis) during the zygotene stage and are held in place along their entire lengths by a protein-DNA structure called the synaptonemal complex (SC) (53). Mutants with defects in homolog prealignment (*chk-2*) or SC formation (*syp-1* and *syp-2*) show embryonic lethality due to chromosome nondysjunction at the first meiotic division (12, 27, 28). Cytological analysis of *Cebrc-2* mutants from the leptotene to diplotene stages of meiosis I failed to detect any morphological abnormality that might suggest homolog alignment or SC defects (data not shown). Consistent with these observations, *Cebrc-2* mutants display normal SC formation and maintenance, as determined by germ line immunostaining with antibodies to the core SC component, SYP-1 (see Fig. S1C in the supplemental material) (12, 27). We conclude that *Cebrc-2* is dispensable for SC formation.

During wild-type meiosis, as nuclei exit the pachytene stage and proceed through the diplotene stage, chromosomes become progressively condensed, and by diakinesis, six distinct DAPI-stained bivalent chromosomes, each corresponding to a pair of homologs held together by a single chiasma, are readily detected in oocyte nuclei (Fig. 4A and B, panel 1). In contrast, *Cebrc-2* mutants display chromosomal abnormalities at diakinesis (Fig. 4B, panel 2). To determine the nature of this defect in *Cebrc-2* mutants, we measured embryonic lethality and an-

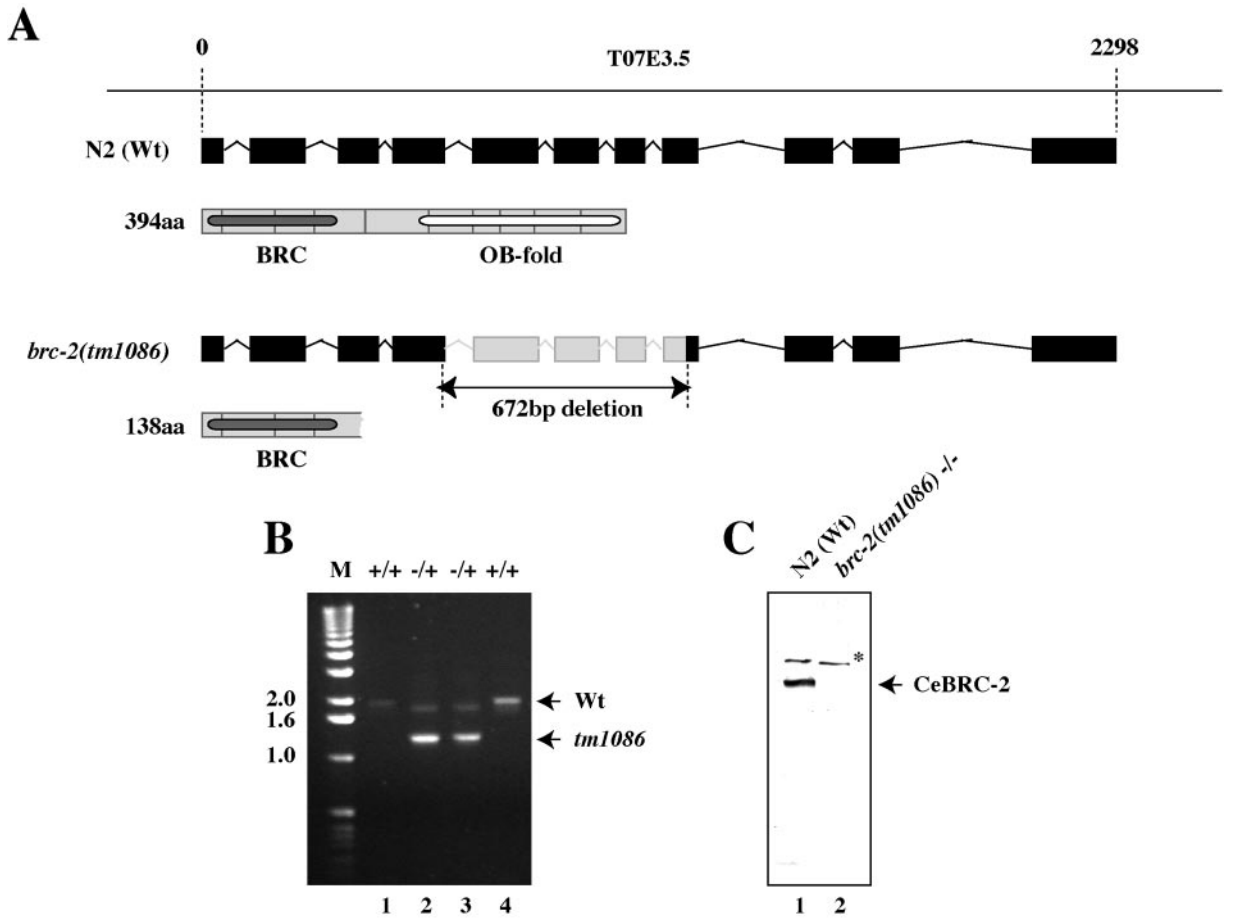

FIG. 3. *Cebrc-2* deletion mutant. (A) Schematics of the gene structure of *Cebrc-2* (T07E3.5) and the predicted protein product for wild-type (Wt) N2 (394-residue protein) and the *brc-2* (*tm1086*) deletion mutant (138-residue predicted protein). *brc-2* (*tm1086*) carries a 672-bp deletion in the *Cebrc-2* gene that removes exons 5 to 8. aa, amino acids. (B) Nested PCR with *Cebrc-2*-specific primers of wild-type N2 (lanes 1 and 4) and *brc-2* (*tm1086*) heterozygotes (lanes 2 and 3) showing the 672-bp deletion. In lanes 2 and 3, the faint band above the *tm1086* deletion product corresponds to the internal PCR product amplified from the wild-type chromosome. (C) Although a 138-residue protein could be expressed from the *brc-2* (*tm1086*) allele, Western blotting with an N-terminus-specific CeBRC-2 antibody failed to detect any protein in a *brc-2* $(tm1086)^{-/-}$ mutant protein compared with full-length CeBRC-2 protein in wild-type N2. The asterisk indicates a nonspecific protein that cross-reacted with the CeBRC-2 antibody.

alyzed chromosome morphology at diakinesis in other mutants known to be affected in meiotic recombination and DNA repair. We also generated double- and triple-mutant combinations with *Cebrc-2* mutants to establish epistatic relationships with *rad-51*, *spo-11*, and *lig-4*. The results of our findings are summarized in Fig. 4A, and representative images of chromosomes at diakinesis in the various mutant combinations are shown in Fig. 4B.

In *Cebrc-2* mutants, chromosomes at diakinesis are highly decondensed and aggregated (Fig. 4A and B, panel 2). Abnormal chromosome aggregates are detected in *Cebrc-2* mutants that manifest fewer than six DAPI-stained structures, varying in number between one and five structures. The fact that we always observed fewer than the expected six DAPI-stained structures might reflect aberrant fusion events between chromosomes but could also correspond to other types of noncovalent entanglements. This phenotype is very similar to that previously observed in *rad-51* mutants (Fig. 4A and B, panel 3), and *Cebrc-2 rad-51* double mutants (Fig. 4A and B, panel 4) display a phenotype very similar to that of the single mutants alone, raising the possibility that these two genes function together in a common pathway (2, 38).

In *spo-11* mutants, 12 DAPI-stained univalents are detected at diakinesis; these arise due to an inability to generate meiotic DSBs that would normally give rise to the chiasmata that physically tether homolog pairs to form bivalents (Fig. 4A and B, panel 5) (15). The absence of chiasmata in *spo-11* mutants leads to a high level of embryonic lethality due to chromosome nondysjunction at the first meiotic division. However, chromosomes do correctly segregate at a low frequency in *spo-11* mutants, resulting in a few viable progeny (Fig. 4A) (15). It was previously shown that *rad-51* mutants are defective for the repair of SPO-11-induced meiotic DSBs (2). We therefore tested whether eliminating meiotic DSBs could suppress the meiotic defect observed in *Cebrc-2* mutants. Indeed, *spo-11 Cebrc-2* double mutants give rise to a low level of viable progeny and possess 12 univalents at diakinesis (Fig. 4A and B,

A

	Genotype	Defect	Live Embryos	% lethality	Number of DAPI stained structures at Diakinesis				
					1-5	6	7-11	12	>12
1.	N2 (Wt)	-	1021 (n = 1023)			n = 52			
2.	*brc-2(tm1086)*	?	0 (n = 798)	100	n = 61				
3.	*rad-51(lg08701)*	HR	0 (n = 624)	100	n = 53				
4.	*brc-2(tm1086); rad-51(lg08701)*	? + HR	0 (n = 1224)	100	n = 28				
5.	*spo-11(ok79)*	Meiotic DSB formation	14 (n = 1878)	99.25				n = 32	
6.	*brc-2(tm1086); spo-11(ok79)*	? + Meiotic DSB formation	9 (n = 1612)	99.44				n = 45	
7.	*lig-4(ok716)*	NHEJ	1094 (n = 1095)	0.10		n = 41			
8.	*brc-2(tm1086); lig-4(RNAi)*	? + NHEJ	0 (n = 567)	100				n = 42	
9.	*rad-51(Ig08701); lig-4(ok716)*	HR + NHEJ	0 (n = 712)	100	n = 31				
10.	*brc-2(tm1086); rad-51(Ig08701) lig-4(RNAi)*	? + HR + NHEJ	0 (n = 522)	100				n = 36	

B

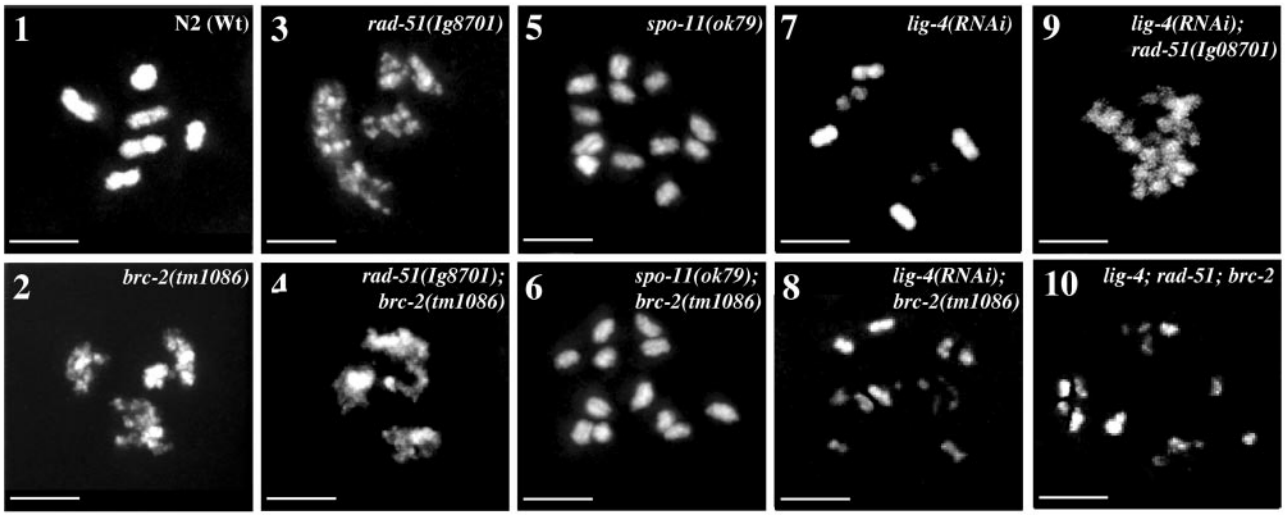

FIG. 4. Embryonic lethality and meiotic DSBR defects in *Cebrc-2* mutants. (A) Table of the number of viable progeny and the number of DAPI-stained structures observed at diakinesis in animals of the indicated genotype (n, number counted). The corresponding defect(s) in meiosis is indicated. N2 (wild type [Wt]) (1) and the *lig-4* mutant (7) have a very low frequency of embryonic lethality and display six bivalent chromosomes at diakinesis. *Cebrc-2* (2), *rad-51* (3), *Cebrc-2 rad-51* (4), and *rad-51 lig-4* (9) mutants fail to produce any viable progeny and display between one and five DAPI-stained structures at diakinesis. *Cebrc-2 lig-4* (8) and *Cebrc-2 rad-51 lig-4* (10) mutants fail to produce any viable progeny and display nine or more DAPI-stained structures at diakinesis. (B) Germ lines from adult hermaphrodites of the indicated genotype were isolated, fixed in paraformaldehyde, and stained with DAPI. A representative projection of a three-dimensional data stack through a single oocyte nucleus at the diakinesis stage of the meiotic prophase is shown. N2 (wild type) (panel 1) and the *lig-4* mutant (7) display six DAPI-stained bivalent chromosomes at diakinesis. Aggregation of chromosomes and chromatin decompaction are detected at diakinesis in *Cebrc-2* (panel 2), *rad-51* (3), *Cebrc-2 rad-51* double (4), and *lig-4* (RNAi) *rad-51* double (9) mutants. Twelve DAPI-stained univalents are seen in *spo-11* (panel 5) and *spo-11 Cebrc-2* double (6) mutants. Twelve or more DAPI-stained structures are seen in *lig-4* (RNAi) *Cebrc-2* double (panel 8) and *Cebrc-2 lig-4* (RNAi) *rad-51* triple (10) mutants. Scale bar, 5 μm.

panel 6). This result implies that the *Cebrc-2* phenotype is caused by a defect in the repair of SPO-11-induced meiotic DSBs.

***Cebrc-2* promotes an alternative DSBR pathway in the absence of HR and NHEJ.** In mutants defective for HR, deletions and translocations arise due to the error-prone repair of DSBs by NHEJ or single-strand annealing (SSA) pathways (17). DSBR by NHEJ involves the direct religation of broken DNA ends and requires the Ku proteins, ligase IV, and a number of other factors. SSA, on the other hand, depends on resection of the DSB to reveal short stretches of homology that flank the break site. Pairing between these homologous sequences followed by ligation leads to deletion of the intervening sequence.

To determine whether the chromosome decompaction and aggregation events that occur in *rad-51* and *Cebrc-2* mutants are a result of repair of meiotic DSBs by NHEJ, we depleted *lig-4* in *Cebrc-2* and *rad-51* mutants by RNAi. We also generated *rad-51 lig-4* double mutants but were unable to generate *lig-4 Cebrc-2* double mutants, as *lig-4* and *Cebrc-2* are tightly linked on chromosome III. *lig-4* mutants or animals depleted of *lig-4* by RNAi [*lig-4* (RNAi)] are homozygous and viable and proceed through meiotic prophase normally, as shown by the presence of six bivalents at diakinesis (Fig. 4A and B, panel 7). RNAi depletion of *lig-4* in *Cebrc-2* mutants significantly reduces the occurrence of the chromosome aggregations that are seen in *Cebrc-2* single mutants. The majority of *Cebrc-2 lig-4* (RNAi) animals possess 12 structurally abnormal univalents at diakinesis, indicating the absence of chiasmata between homolog pairs and aberrant chromosome fusions (Fig. 4A and B, panel 8, and data not shown). In a few cases, we observed fewer

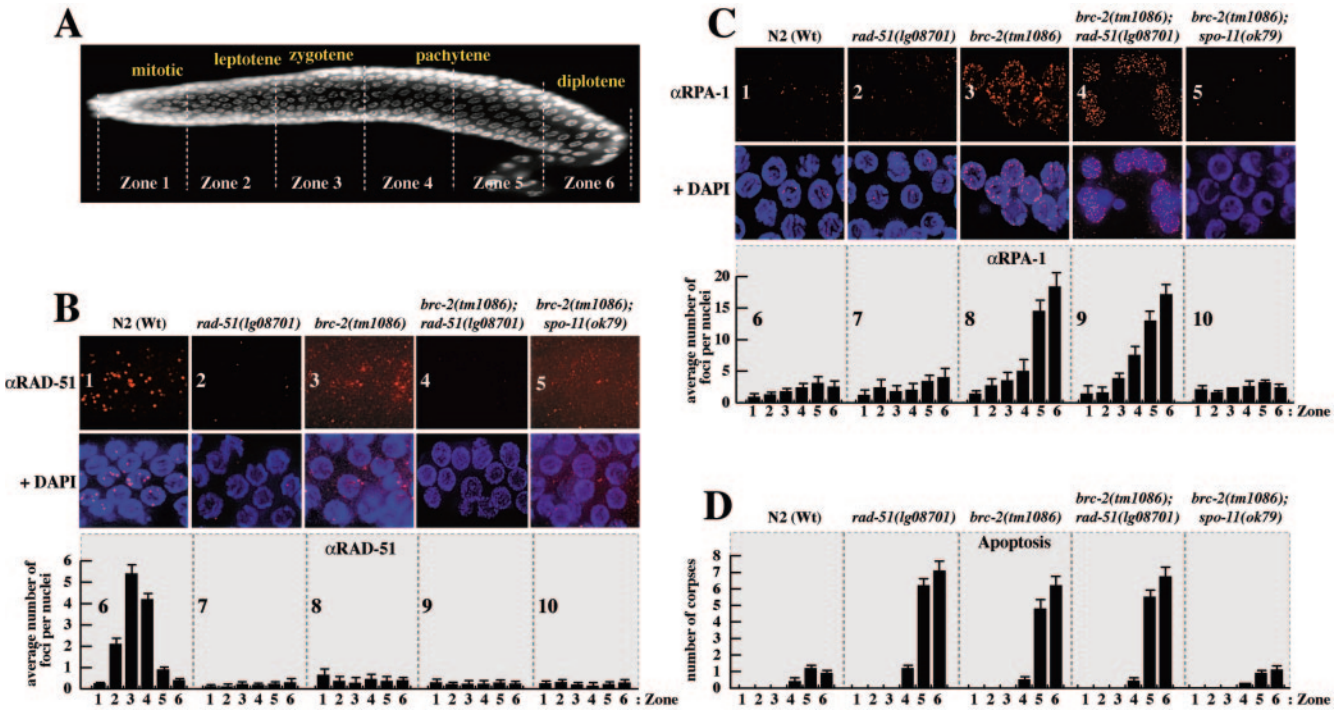

FIG. 5. Loss of *Cebrc-2* disrupts RAD-51 localization and results in RPA-1 accumulation at DSBs. (A) Low-magnification images of a wild-type germ line stained with DAPI depicting the six zones in which RAD-51, RPA-1, and apoptosis are quantitated. (B) Representative images of RAD-51 staining in midpachytene nuclei (panels 1 to 5) and quantitation of RAD-51 foci in the six zones of the germ line (6 to 10) for the indicated genotypes. Wt, wild type. (C) Representative images of RPA-1 staining in late-pachytene nuclei (panels 1 to 5) and quantitation of RPA-1 foci in the six zones of the germ line (6 to 10) for the indicated genotypes. (D) Increased apoptotic corpses in *rad-51*, *Cebrc-2*, and *Cebrc-2 rad-51* double mutants. Corpses were counted in each of the six zones and are shown for the indicated genotypes as previously described (5).

than 12 DAPI-stained structures, and in others, we detected fragments of DNA leading to a total of more than 12 DAPI-stained structures at diakinesis (Fig. 4A). These observations suggest that NHEJ is at least partially responsible for the aberrant chromosome aggregates that occur in the absence of *Cebrc-2*. Surprisingly, in *rad-51 lig-4* (RNAi) and *rad-51 lig-4* double mutants, in which both HR (*rad-51*) and NHEJ (*lig-4*) are defective, chromosome aggregates still occur (Fig. 4A and B, panel 9). These results suggest that an alternative DSBR pathway is still operable in these mutants. Given the difference between *Cebrc-2 lig-4* (RNAi) and *rad-51 lig-4* mutants, we reasoned that *Cebrc-2* may be required to promote the alternative DSBR pathway responsible for the chromosome fusions observed in the absence of HR (*rad-51*) and NHEJ (*lig-4*). To test this possibility, we depleted *lig-4* in *Cebrc-2 rad-51* mutants. *Cebrc-2 rad-51 lig-4* (*RNAi*) mutants display mainly 12 nonfused but structurally abnormal univalents at diakinesis, similar to *Cebrc-2 lig-4* (RNAi) mutants (Fig. 4B, panel 10). Thus, elimination of both *lig-4* and *Cebrc-2* is required to abolish the repair of meiotic DSBs that result in aberrant chromosome aggregates at diakinesis in *rad-51* mutants.

Together, these data indicate that SPO-11-induced meiotic DSBs form normally in *Cebrc-2* and *rad-51* mutants but that, due to a defect in the HR pathway, meiotic DSBs are aberrantly repaired by NHEJ and an alternative DSBR pathway that requires *Cebrc-2*.

Aberrant RAD-51 localization and accumulation of RPA-1 at meiotic DSBs in *Cebrc-2* mutants. To examine the basis of the HR defect in *Cebrc-2* mutants, we performed germ line immunostaining with antibodies to RAD-51 and RPA-1 to monitor the recruitment and formation of RAD-51 and RPA-1 foci at meiotic DSBs. Since the meiotic prophase is spatially organized in a distal-to-proximal manner in the *C. elegans* germ line, we assessed the timing of the appearance and disappearance of these foci during the meiotic prophase by dividing the germ line into six zones and quantitating the number of foci per nucleus in each zone (Fig. 5A). In wild-type meiosis, RAD-51 foci appear in the transition zone (which contains nuclei in the leptotene and zygotene stages), become abundant from the late zygotene to the midpachytene stages, and are lost from the late pachytene stage onward (Fig. 5B, panels 1 and 6) (2, 12). These foci correspond to sites of meiotic DSBs as they are abolished in *spo-11* mutants (2). In contrast to what is observed in the wild type, RAD-51 focus formation is dramatically reduced in the nuclei of *Cebrc-2* mutants (Fig. 5B, panels 3 and 8) and is completely absent in *rad-51* mutants (Fig. 5B, panels 2 and 7), *Cebrc-2 rad-51* double mutants (Fig. 5B, panels 4 and 9), and *Cebrc-2 spo-11* double mutants (Fig. 5B, panels 5 and 10). Instead, RAD-51 staining is both cytoplasmic and nuclear in *Cebrc-2* mutants and *Cebrc-2 spo-11* mutants (Fig. 5B, panels 3 and 5).

Since RPA has been shown to be one of the first proteins to associate with resected DSBs in yeast cells (33), we next performed germ line immunostaining with RPA-1 antibodies. In the wild type, RPA-1 is largely diffuse and weakly nuclear in the early prophase, increasing in intensity in the diplotene

stage and diakinesis (data not shown), with 2.8 ± 1.4 (mean ± standard deviation) RPA-1 foci per nucleus (Fig. 5C, panels 1 and 6). In striking contrast, RPA-1 foci are dramatically increased from the late pachytene stage onward in *Cebrc-2* mutants, with 16.4 ± 6.2 RPA-1 foci per nucleus (Fig. 5C, panels 3 and 8). Surprisingly, *rad-51* mutants display wild-type levels of RPA-1 staining (Fig. 5C, panels 2 and 7), whereas *Cebrc-2 rad-51* double mutants exhibit extensive accumulation of RPA-1 foci from the late pachytene stage onward, similar to *Cebrc-2* mutants (Fig. 5C, panels 4 and 9). To determine whether meiotic DSBs are required for RPA-1 accumulation in *Cebrc-2* mutants, we generated *Cebrc-2 spo-11* double mutants. RPA-1 failed to accumulate in *Cebrc-2 spo-11* double mutants, implying that RPA-1 accumulates at sites of meiotic DSBs in *Cebrc-2* mutants (Fig. 5C, panels 5 and 10). Since *rad-51* mutants do not accumulate RPA-1 staining, these data also suggest that *Cebrc-2* can function independently of *rad-51* to prevent the accumulation of RPA-1 at meiotic DSBs.

***Cebrc-2* is dispensable for sensing DNA damage and checkpoint activation.** The defects observed in *Cebrc-2* mutants may also reflect roles in sensing the presence of DNA damage or activating the DNA damage checkpoint (8). To test this possibility, we measured apoptosis of cells in the late pachytene stage and cell cycle arrest in the mitotic zone of the germ line, both of which require an intact checkpoint response (5). Although we observed profound differences between *rad-51* and *Cebrc-2* mutants in RPA-1 accumulation at meiotic DSBs, both mutants exhibited *spo-11*-dependent increases in apoptosis in the late pachytene stage compared to the wild type (Fig. 5D) (2). Moreover, *Cebrc-2 rad-51* double mutants exhibited similar increases in apoptosis in the late pachytene stage compared to single mutants alone (Fig. 5D).

In response to treatment with hydroxyurea or gamma irradiation, mitotic nuclei at the distal end of the germ line of *Cebrc-2* mutants undergo normal cell cycle arrest, whereas *rad-5* checkpoint-defective mutants fail to arrest in response to both treatments (see Fig. S1D in the supplemental material) (1, 5). Together, these results imply that *Cebrc-2* is dispensable for the intra-S-phase, G_2-M phase, and pachytene checkpoints that induce cell cycle arrest and apoptosis.

***Cebrc-2* is required for RAD-51 focus formation in response to DNA damage.** In the wild type, germ line nuclei accumulate both RAD-51 and RPA-1 foci at sites of DSBs following treatment with gamma irradiation (Fig. 6A, panels 1 and 4, and 6B, panels 1 and 4). In contrast, RAD-51 focus formation is impaired in *Cebrc-2* mutants after exposure to gamma irradiation, with increased levels of RAD-51 being seen in the cytoplasm (Fig. 6A, panels 3 and 4). In addition, the number of RPA-1 foci is increased compared with that in nonirradiated animals (Fig. 6B, panels 3 and 4). Since RPA-1 foci accumulate to approximately wild-type levels in *rad-51* mutants following irradiation treatment (Fig. 6B, panels 2 and 4), we conclude that *Cebrc-2* performs *rad-51*-independent functions in preventing the accumulation of RPA-1 at both meiotic and radiation-induced DSBs.

To further test whether CeBRC-2 is required for the recruitment of nuclear RAD-51 to processed DSBs, we adopted a dominant-negative approach to inhibit CeBRC-2 function in wild-type animals. Peptides corresponding to BRC3 or BRC4 motifs in human BRCA2 efficiently block nucleoprotein filament formation by RAD51 in vitro (14). Therefore, we reasoned that peptides corresponding to the BRC motif in CeBRC-2 may also block RAD-51 focus formation at DSBs by directly competing with endogenous CeBRC-2 for RAD-51 binding. To test this possibility, we synthesized a wild-type 69-amino-acid peptide containing the conserved 25-amino-acid BRC motif (BRC_Wt) that is able to bind efficiently to RAD-51 and a mutant peptide with a 7-amino-acid deletion (ΔS36-R42) in the most highly conserved STAAGIR sequence that abolishes binding to RAD-51 (BRC_Mut) (Fig. 6C) (4, 14). Injection of the BRC_Wt peptide into the germ lines of wild-type (N2) worms blocks RAD-51 focus formation at sites of radiation-induced DNA damage in all germ lines injected ($n = 25$) (Fig. 6D). However, injection of the BRC_Mut peptide at up to five times the concentration of the wild-type peptide had no effect on RAD-51 focus formation at sites of DNA damage ($n = 25$) (Fig. 6D and data not shown). These results suggest that the BRC motif alone can function in a dominant-negative manner to block RAD-51 focus formation in vivo in wild-type animals.

CeBRC-2 forms foci at radiation-induced DSBs independent of *rad-51*. We next performed CeBRC-2 immunostaining of wild-type (N2) germ lines to determine whether CeBRC-2 localizes to radiation-induced DSBs. In nonirradiated wild-type (N2) animals, CeBRC-2 is diffuse and detected at very low levels in nuclei (Fig. 7, panel 1). However, after radiation treatment, germ line nuclei accumulate a large number of discrete foci concordant with DNA (Fig. 7, panel 2). No signal is detected in *Cebrc-2* mutants, demonstrating that the focus formation observed in wild-type animals after radiation treatment is specific to CeBRC-2 (Fig. 7, panel 3). These results imply that CeBRC-2 localizes to presumptive sites of DNA damage after radiation treatment.

Since it was not previously possible to assess the role of RAD51 in recruiting BRCA2 to sites of DNA damage, as the disruption of *RAD51* in mice results in early embryonic lethality and cell lines derived from these mice do not survive in cultures (24, 43), we performed CeBRC-2 immunostaining of *rad-51* mutant germ lines. Surprisingly, we found that CeBRC-2 foci still form after radiation treatment in *rad-51* mutants (Fig. 7, panel 4), suggesting that CeBRC-2 can localize to presumptive sites of DNA damage independent of *rad-51*.

DISCUSSION

BRCA2 homolog in *C. elegans*. In a screen for RAD-51-interacting proteins in *C. elegans*, we identified CeBRC-2, a BRCA2-related protein that contains a single BRC motif and a single OB fold domain. Although CeBRC-2 is only a little over 1/10th the size of human BRCA2, they share many functional similarities. We have shown that CeBRC-2 interacts directly with RAD-51 in vitro and in vivo via its BRC motif and preferentially binds to ssDNA through its OB fold domain. We find that disruption of *Cebrc-2* confers meiotic and radiation-induced DNA repair defects similar to mutations in *rad-51* and consistent with previous studies of BRCA2-like proteins in *U. maydis* and *A. thaliana* (21, 41). By exploiting the spatial organization of meiotic prophase within the *C. elegans* adult hermaphrodite germ line, we have dissected the role of *Cebrc-2*

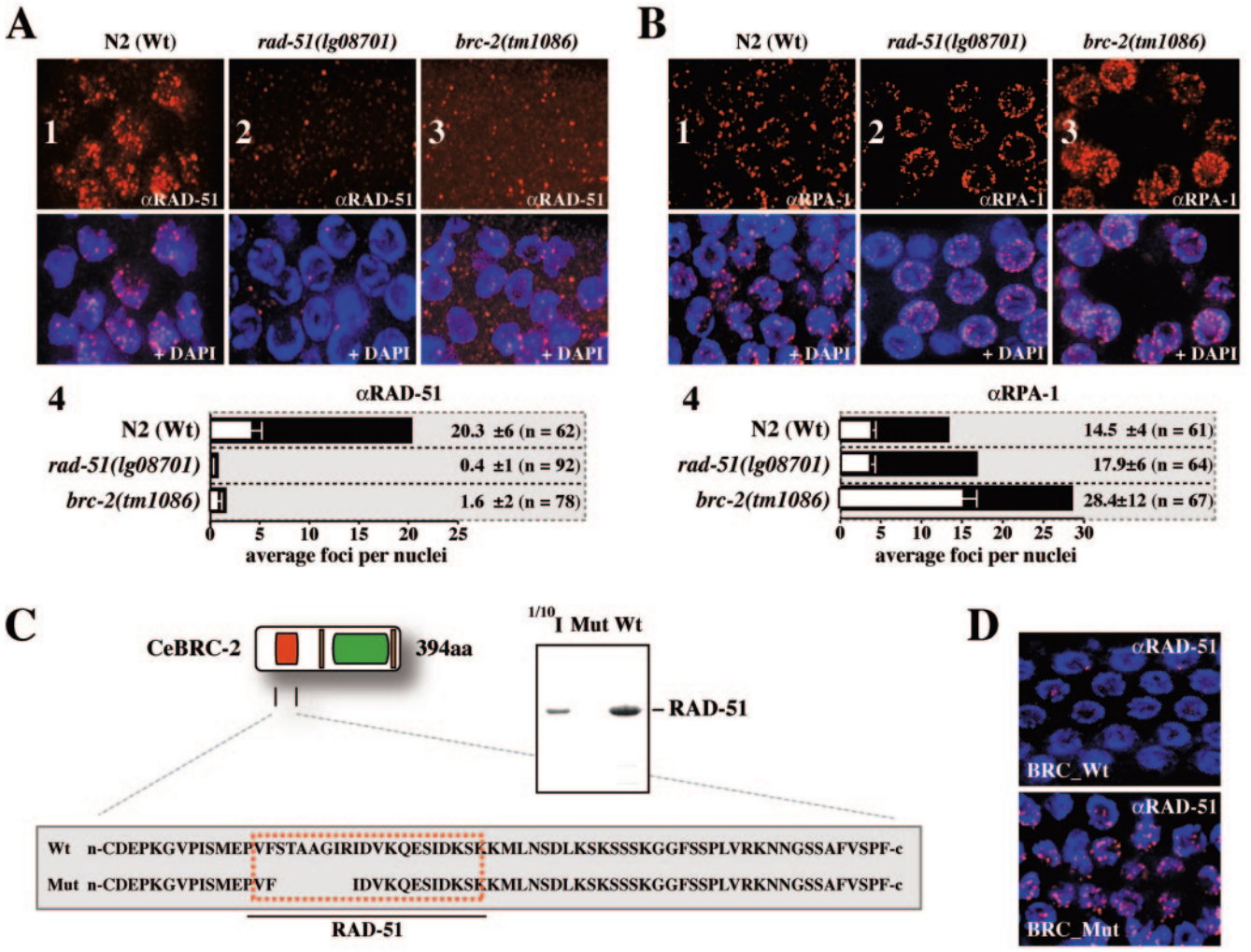

FIG. 6. Radiation-induced defects in *Cebrc-2* mutants. RAD-51 and RPA-1 staining reveal radiation-induced DSBR defects in *Cebrc-2* mutants and following microinjection of dominant-negative BRC peptides into N2 (wild type [Wt]). Immunostaining was performed for RAD-51 (A) and RPA-1 (B) on germ lines of the indicated genotypes at 4 h after treatment with 75 Gy of gamma irradiation. The average number of RAD-51 and RPA-1 foci per nucleus is graphically represented (n, number of nuclei counted) The average number of foci per nucleus in the absence of gamma irradiation is shown by the white bars. (C) Schematic of wild-type (BRC_Wt) and mutant (BRC_Mut) BRC peptides. The mutant BRC peptide has a deletion of seven residues within the RAD-51 interaction domain. The BRC_Wt peptide efficiently pulls down RAD-51 from whole worm extracts, but the BRC_Mut peptide is defective for RAD-51 binding. Peptide pull-down assay samples and 1/10 the input ($^{1/10}$I) were subjected to Western blotting with a RAD-51 antibody. (D) Representative images of RAD-51 staining in germ lines injected with BRC_Wt and BRC_Mut peptides. Each peptide (1 mg/ml) was microinjected into the germ line of 25 N2 (wild-type) animals. At 2 h after injection, animals were exposed to 75 Gy of gamma irradiation. At 4 h after irradiation, germ line nuclei were fixed and immunostained with RAD-51 antibody.

during the meiotic prophase. While the SC forms normally in *Cebrc-2* mutants, meiotic and radiation-induced DSBs are inefficiently repaired due to a defect in HR. Consistent with a role in DSBR, CeBRC-2 forms foci after radiation treatment at presumptive sites of DNA damage. We have also shown that sensing of DNA damage appears to occur normally in *Cebrc-2* mutants, as mitotic germ line nuclei undergo cell cycle arrest in response to gamma irradiation and hydroxyurea, and nuclei with persistent meiotic DSBs are eliminated by apoptosis.

CeBRC-2 regulates RAD-51 during HR. Our findings suggest roles for CeBRC-2 at two steps during the repair of meiotic and radiation-induced DSBs by HR: (i) it is required for efficient transport or retention of RAD-51 in the nucleus; and (ii) it is required for the targeting of RAD-51 to DSBs (Fig. 8). First, our observation that *Cebrc-2* mutants have detectable RAD-51 in the cytoplasm by immunofluorescence analysis suggests that *Cebrc-2* may be required for the efficient nuclear localization or nuclear retention of RAD-51. These possibilities will require further analysis to confirm but are consistent with previous findings that RAD51 accumulates in the cytoplasm of CAPAN-1 cells, which carry a truncating mutation in BRCA2 (14). *C. elegans* RAD-51 lacks an NLS; therefore, its entry into the nucleus may depend on an association with CeBRC-2, which possesses two NLSs flanking its OB fold domain. Second, previous studies with *C. elegans* demonstrated that RAD-51 foci form in the early meiotic prophase at sites of meiotic DSBs that are generated by the action of SPO-11 (2, 15). Since meiotic RAD-51 foci fail to form in *brc-2* mutants,

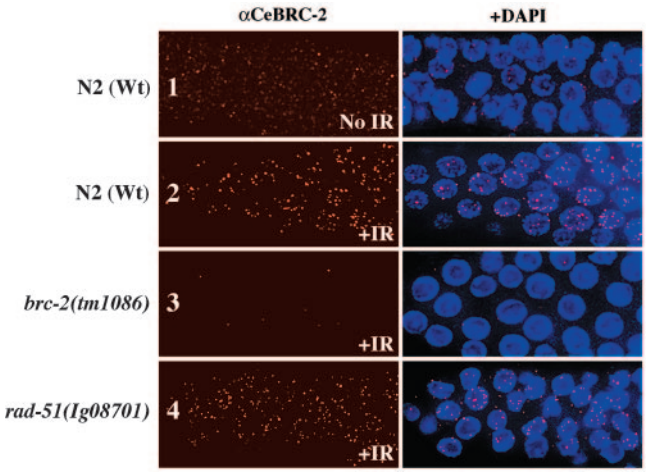

FIG. 7. CeBRC-2 forms foci after DNA damage independent of *rad-51*. Representative images show CeBRC-2 staining in mitotic germ line nuclei of the indicated genotypes before and 4 h after treatment with 75 Gy of gamma irradiation (IR). Wt, wild type.

we propose that CeBRC-2 is required for recruiting RAD-51 to DSBs. Our observation that germ line injection of a BRC peptide acts in a dominant-negative manner to block RAD-51 focus formation in response to DNA damage suggests a role for CeBRC-2 in targeting RAD-51 to both meiotic and radiation-induced DSBs. Third, CeBRC-2 forms foci after radiation treatment, suggesting that it may localize to sites of active DNA repair in vivo. Together, these data support a role for CeBRC-2 in the recruitment of RAD-51 to processed DSBs in vivo (Fig. 8). Currently, we cannot exclude the possibility that the defect in RAD-51 focus formation in *Cebrc-2* mutants may also reflect roles for CeBRC-2 in stimulating RAD-51 nucleoprotein filament formation, stabilizing the filament once it has formed and/or regulating the strand exchange activity of RAD-51 (3). Future studies with recombinant CeBRC-2 and RAD-51 in vitro may shed light on these possibilities.

RAD-51-independent roles of CeBRC-2. A direct comparison of the roles of *RAD51* and *BRCA2* in DSBR has not been possible in mice due to early embryonic lethality (13, 24, 26, 39, 42, 43). Our analysis of *rad-51* and *Cebrc-2* mutants in *C. elegans* reveals unexpected phenotypic differences that suggest *rad-51*-dependent and -independent actions of CeBRC-2 in DNA repair processes.

Our data suggest two novel roles for *Cebrc-2* independent of *rad-51*: (i) promoting an alternative DSBR process that is distinct from NHEJ and (ii) preventing the accumulation of RPA-1 at DSBs (Fig. 8). First, we have shown that chromosome aggregates detected at diakinesis in both *rad-51* and *Cebrc-2* mutants arise due to aberrant repair of meiotic DSBs. Chromosome aggregates still occur in *rad-51 lig-4* double mutants (defective in HR and NHEJ), suggesting that an alternative DSBR pathway is still functional in these mutants. We show that the alternative DSBR pathway requires *Cebrc-2*, as revealed by the significant reduction in abnormal chromosome aggregates in *Cebrc-2 lig-4* (RNAi) and *Cebrc-2 rad-51 lig-4* (RNAi) mutants. We propose that *Cebrc-2* normally functions in the HR pathway but can promote an alternative mechanism of DSBR when HR and NHEJ are compromised. One possibility is that CeBRC-2 is required for SSA. The budding yeast protein Rad52 is essential for HR and SSA and has many functional similarities with CeBRC-2 in DNA repair (25). Like CeBRC-2, Rad52 binds to ssDNA, interacts directly with Rad51, and is required for Rad51 focus formation at sites of DSBs (48). Rad52 also functions independently of Rad51 in DSBR by SSA, where it promotes homologous pairing between short stretches of ssDNA that flank the break site. Given

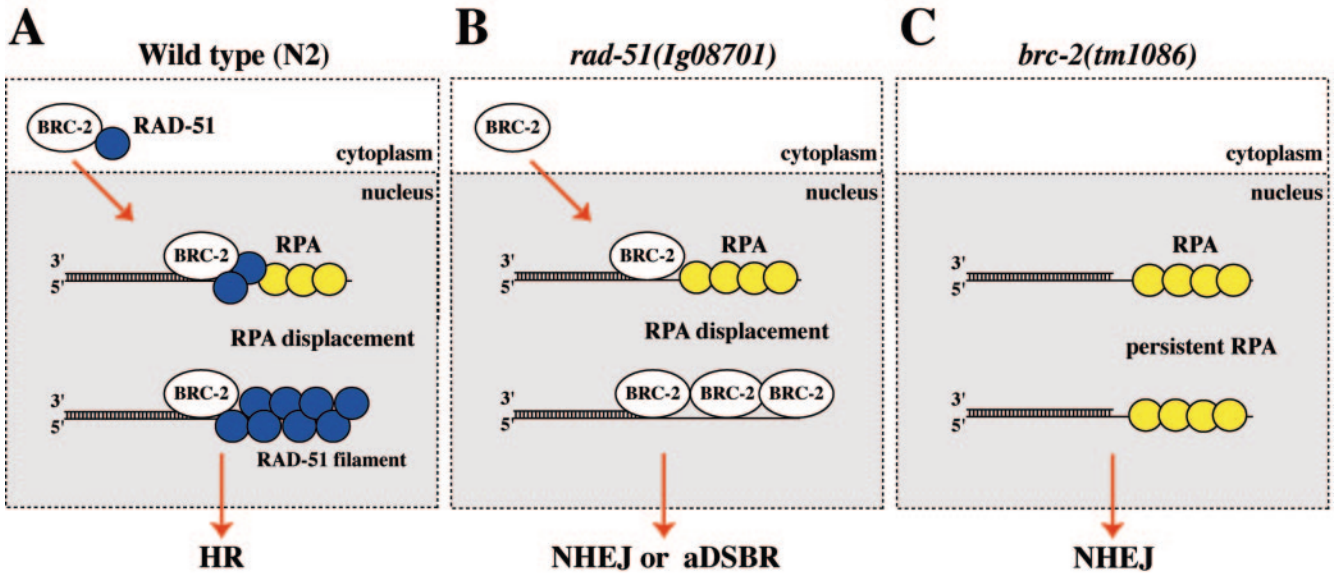

FIG. 8. Possible roles of CeBRC-2 in DSBR. (A) In wild-type (N2) animals, CeBRC-2 functions in DSBs through HR by transporting RAD-51 into the nucleus and targeting RAD-51 to processed DBSs. (B) In *rad-51* mutants (defective for HR), CeBRC-2 may displace or prevent the accumulation of RPA-1 at resected DSBs. CeBRC-2 can also promote an alternative DSBR (aDSBR) pathway distinct from NHEJ. (C) In *Cebrc-2* mutants (defective for HR and aDSBR), RPA-1 persists or accumulates at DSBs, and repair ensues by NHEJ.

the central importance of Rad52 in yeast DSBR, it is perhaps surprising that the genomes of *C. elegans*, *Drosophila melanogaster*, and *A. thaliana* lack a Rad52 homolog. It is therefore tempting to speculate that CeBRC-2 may have taken over the role of Rad52 in the SSA pathway. However, at this point we cannot exclude the possibility that CeBRC-2 may regulate a Rad52-like activity required for SSA or may function in an alternative DSBR pathway other than SSA. Although *BRCA2*-defective mammalian cells can perform SSA reactions (44), this function may be redundant with that of *RAD52*. In future studies, it will be important to define the precise role of CeBRC-2 in the alternative DSBR pathway.

Second, our analyses reveal that *Cebrc-2* mutants accumulate RPA-1 at DSBs during the meiotic prophase and following exposure to gamma irradiation. Since this phenotype does not occur in wild-type animals and is suppressed by a mutation in *spo-11*, it is likely that this defect reflects recombination intermediates (resected DSBs decorated with RPA-1) that persist in the absence of efficient DNA repair via HR. However, this simple interpretation does not account for the fact that *rad-51* mutants do not accumulate RPA-1 at DSBs yet are clearly impaired for meiotic and radiation-induced DSBR by HR. Our observation that radiation-induced CeBRC-2 foci still form in *rad-51* mutants supports a model in which CeBRC-2 can perform actions at sites of DNA damage in the absence of *rad-51* (Fig. 8). One possibility is that meiotic and radiation-induced DSBs become hyperresected in *Cebrc-2* mutants, resulting in extended regions of ssDNA bound by RPA-1. Alternatively, CeBRC-2 may displace RPA-1 at processed breaks, an activity that can still occur in wild-type and *rad-51* mutants. Consistent with these observations, *Brca2*-defective spermatocytes also exhibit significantly elevated levels of RPA staining (40). Furthermore, we have shown that CeBRC-2 binds preferentially to ssDNA in vitro and may therefore play a role in displacing RPA-1 at resected DSBs by competing for ssDNA binding (Fig. 8). Our observation that the CeBRC-2 fragment containing amino acids 114 to 394 and RPA-1 can weakly interact with each other in the yeast-two hybrid system (Fig. 2A) raises the possibility that CeBRC-2 may bind to and actively release RPA-1 from processed breaks. Unfortunately, it has not been possible to test whether CeBRC-2 can displace RPA from ssDNA in vitro, as only two of the three *C. elegans* RPA subunits are presently known.

CeBRC-2 is amenable to biochemical analysis. Investigation of the biochemical activities of human BRCA2 has been hampered by the inability to express and purify full-length protein to sufficient levels due to problems with its size, solubility, and nonspecific degradation. Full-length CeBRC-2 can be expressed and purified in large quantities (Fig. 2E and data not shown), an important development toward an in vitro system for elucidating BRCA2-related protein function during HR. Taken together with the fact that other HR cofactors exist in *C. elegans*, our findings suggest that future biochemical and structural studies of CeBRC-2 are likely to provide important insights into its role in repair and recombination.

In conclusion, *C. elegans* possesses a BRCA2-related protein that regulates RAD-51 during HR and promotes an alterative DSBR pathway in the absence of *rad-51* and distinct from NHEJ. Given the functional similarities between CeBRC-2 and BRCA2, it is likely that further study of the *C. elegans* protein will provide mechanistic insight into the role of human BRCA2 in DSBR processes.

ACKNOWLEDGMENTS

We thank the National Bioresource Project for the Nematode (Shohei Mitani), the *Caenorhabditis* Genetics Center, and Alan Coulson for providing *C. elegans* strains and cosmids. We also thank Arno Alpi and Anton Gartner for kindly providing antibodies to RAD-51 and RPA-1 and Anne Villeneuve and Monica Colaiacovo for kindly providing antibody to SYP-1. In addition, we thank Juliet Reid, Alison Schuldt, John Diffley, Jesper Svejstrup, and Tomas Lindahl for comments on the manuscript. We are also grateful to members of the London Research Institute, Cancer Research UK, for helpful discussions.

This work was funded by Cancer Research UK.

REFERENCES

1. **Ahmed, S., A. Alpi, M. O. Hengartner, and A. Gartner.** 2001. *C. elegans* RAD-5/CLK-2 defines a new DNA damage checkpoint protein. Curr. Biol. **11:**1934–1944.
2. **Alpi, A., P. Pasierbek, A. Gartner, and J. Loidl.** 2003. Genetic and cytological characterization of the recombination protein RAD-51 in *Caenorhabditis elegans*. Chromosoma **112:**6–16.
3. **Baumann, P., and S. C. West.** 1998. Role of the human RAD51 protein in homologous recombination and double-stranded-break repair. Trends Biochem. Sci. **23:**247–251.
4. **Bignell, G., G. Micklem, M. R. Stratton, A. Ashworth, and R. Wooster.** 1997. The BRC repeats are conserved in mammalian BRCA2 proteins. Hum. Mol. Genet. **6:**53–58.
5. **Boulton, S. J., A. Gartner, J. Reboul, P. Vaglio, N. Dyson, D. E. Hill, and M. Vidal.** 2002. Combined functional genomic maps of the *C. elegans* DNA damage response. Science **295:**127–131.
6. **Boulton, S. J., J. S. Martin, J. Polanowska, D. E. Hill, A. Gartner, and M. Vidal.** 2004. BRCA1/BARD1 orthologs required for DNA repair in *Caenorhabditis elegans*. Curr. Biol. **14:**33–39.
7. **Brenner, S.** 1974. The genetics of *Caenorhabditis elegans*. Genetics **77:**71–94.
8. **Chen, C., and R. D. Kolodner.** 1999. Gross chromosomal rearrangements in *Saccharomyces cerevisiae* replication and recombination defective mutants. Nat. Genet. **23:**81–85.
9. **Chen, C. F., P. L. Chen, Q. Zhong, Z. D. Sharp, and W. H. Lee.** 1999. Expression of BRC repeats in breast cancer cells disrupts the BRCA2-Rad51 complex and leads to radiation hypersensitivity and loss of G(2)/M checkpoint control. J. Biol. Chem. **274:**32931–32935.
10. **Chen, J., D. P. Silver, D. Walpita, S. B. Cantor, A. F. Gazdar, G. Tomlinson, F. J. Couch, B. L. Weber, T. Ashley, D. M. Livingston, and R. Scully.** 1998. Stable interaction between the products of the BRCA1 and BRCA2 tumor suppressor genes in mitotic and meiotic cells. Mol. Cell **2:**317–328.
11. **Chen, P. L., C. F. Chen, Y. Chen, J. Xiao, Z. D. Sharp, and W. H. Lee.** 1998. The BRC repeats in BRCA2 are critical for RAD51 binding and resistance to methyl methanesulfonate treatment. Proc. Natl. Acad. Sci. USA **95:**5287–5292.
12. **Colaiacovo, M. P., A. J. MacQueen, E. Martinez-Perez, K. McDonald, A. Adamo, A. La Volpe, and A. M. Villeneuve.** 2003. Synaptonemal complex assembly in *C. elegans* is dispensable for loading strand-exchange proteins but critical for proper completion of recombination. Dev. Cell **5:**463–474.
13. **Connor, F., D. Bertwistle, P. J. Mee, G. M. Ross, S. Swift, E. Grigorieva, V. L. Tybulewicz, and A. Ashworth.** 1997. Tumorigenesis and a DNA repair defect in mice with a truncating Brca2 mutation. Nat. Genet. **17:**423–430.
14. **Davies, A. A., J. Y. Masson, M. J. McIlwraith, A. Z. Stasiak, A. Stasiak, A. R. Venkitaraman, and S. C. West.** 2001. Role of BRCA2 in control of the RAD51 recombination and DNA repair protein. Mol. Cell **7:**273–282.
15. **Dernburg, A. F., K. McDonald, G. Moulder, R. Barstead, M. Dresser, and A. M. Villeneuve.** 1998. Meiotic recombination in *C. elegans* initiates by a conserved mechanism and is dispensable for homologous chromosome synapsis. Cell **94:**387–398.
16. **Howlett, N. G., T. Taniguchi, S. Olson, B. Cox, Q. Waisfisz, C. De Die-Smulders, N. Persky, M. Grompe, H. Joenje, G. Pals, H. Ikeda, E. A. Fox, and A. D. D'Andrea.** 2002. Biallelic inactivation of BRCA2 in Fanconi anemia. Science **297:**606–609.
17. **Jeggo, P. A.** 1998. DNA breakage and repair. Adv. Genet. **38:**185–218.
18. **Keeney, S., C. N. Giroux, and N. Kleckner.** 1997. Meiosis-specific DNA double-strand breaks are catalyzed by Spo11, a member of a widely conserved protein family. Cell **88:**375–384.
19. **Kerr, P., and A. Ashworth.** 2001. New complexities for BRCA1 and BRCA2. Curr. Biol. **11:**R668–R676.
20. **Khanna, K. K., and S. P. Jackson.** 2001. DNA double-strand breaks: signaling, repair and the cancer connection. Nat. Genet. **27:**247–254.
21. **Kojic, M., C. F. Kostrub, A. R. Buchman, and W. K. Holloman.** 2002. BRCA2 homolog required for proficiency in DNA repair, recombination, and genome stability in *Ustilago maydis*. Mol. Cell **10:**683–691.

22. **Kojic, M., H. Yang, C. F. Kostrub, N. P. Pavletich, and W. K. Holloman.** 2003. The BRCA2-interacting protein DSS1 is vital for DNA repair, recombination, and genome stability in *Ustilago maydis*. Mol. Cell **12:**1043–1049.
23. **Li, S., C. M. Armstrong, N. Bertin, H. Ge, S. Milstein, M. Boxem, P. O. Vidalain, J. D. Han, A. Chesneau, T. Hao, D. S. Goldberg, N. Li, M. Martinez, J. F. Rual, P. Lamesch, L. Xu, M. Tewari, S. L. Wong, L. V. Zhang, G. F. Berriz, L. Jacotot, P. Vaglio, J. Reboul, T. Hirozane-Kishikawa, Q. Li, H. W. Gabel, A. Elewa, B. Baumgartner, D. J. Rose, H. Yu, S. Bosak, R. Sequerra, A. Fraser, S. E. Mango, W. M. Saxton, S. Strome, S. Van Den Heuvel, F. Piano, J. Vandenhaute, C. Sardet, M. Gerstein, L. Doucette-Stamm, K. C. Gunsalus, J. W. Harper, M. E. Cusick, F. P. Roth, D. E. Hill, and M. Vidal.** 2004. A map of the interactome network of the metazoan *C. elegans*. Science **303:**540–543.
24. **Lim, D. S., and P. Hasty.** 1996. A mutation in mouse rad51 results in an early embryonic lethal that is suppressed by a mutation in p53. Mol. Cell. Biol. **16:**7133–7143.
25. **Lo, T., L. Pellegrini, A. R. Venkitaraman, and T. L. Blundell.** 2003. Sequence fingerprints in BRCA2 and RAD51: implications for DNA repair and cancer. DNA Repair (Amsterdam) **2:**1015–1028.
26. **Ludwig, T., D. L. Chapman, V. E. Papaioannou, and A. Efstratiadis.** 1997. Targeted mutations of breast cancer susceptibility gene homologs in mice: lethal phenotypes of Brca1, Brca2, Brca1/Brca2, Brca1/p53, and Brca2/p53 nullizygous embryos. Genes Dev. **11:**1226–1241.
27. **MacQueen, A. J., M. P. Colaiacovo, K. McDonald, and A. M. Villeneuve.** 2002. Synapsis-dependent and -independent mechanisms stabilize homolog pairing during meiotic prophase in *C. elegans*. Genes Dev. **16:**2428–2442.
28. **MacQueen, A. J., and A. M. Villeneuve.** 2001. Nuclear reorganization and homologous chromosome pairing during meiotic prophase require *C. elegans* chk-2. Genes Dev. **15:**1674–1687.
29. **Marmorstein, L. Y., T. Ouchi, and S. A. Aaronson.** 1998. The BRCA2 gene product functionally interacts with p53 and RAD51. Proc. Natl. Acad. Sci. USA **95:**13869–13874.
30. **Marston, N. J., W. J. Richards, D. Hughes, D. Bertwistle, C. J. Marshall, and A. Ashworth.** 1999. Interaction between the product of the breast cancer susceptibility gene BRCA2 and DSS1, a protein functionally conserved from yeast to mammals. Mol. Cell. Biol. **19:**4633–4642.
31. **McIlwraith, M. J., E. Van Dyck, J. Y. Masson, A. Z. Stasiak, A. Stasiak, and S. C. West.** 2000. Reconstitution of the strand invasion step of double-strand break repair using human Rad51 Rad52 and RPA proteins. J. Mol. Biol. **304:**151–164.
32. **Moynahan, M. E., A. J. Pierce, and M. Jasin.** 2001. BRCA2 is required for homology-directed repair of chromosomal breaks. Mol. Cell **7:**263–272.
33. **Paques, F., and J. E. Haber.** 1999. Multiple pathways of recombination induced by double-strand breaks in *Saccharomyces cerevisiae*. Microbiol. Mol. Biol. Rev. **63:**349–404.
34. **Pellegrini, L., D. S. Yu, T. Lo, S. Anand, M. Lee, T. L. Blundell, and A. R. Venkitaraman.** 2002. Insights into DNA recombination from the structure of a RAD51-BRCA2 complex. Nature **420:**287–293.
35. **Polanowska, J., J. S. Martin, R. Fisher, T. Scopa, I. Rae, and S. J. Boulton.** 2004. Tandem immunoaffinity purification of protein complexes from *Caenorhabditis elegans*. BioTechniques **36:**778–780, 782.
36. **Praitis, V., E. Casey, D. Collar, and J. Austin.** 2001. Creation of low-copy integrated transgenic lines in *Caenorhabditis elegans*. Genetics **157:**1217–1226.
37. **Rahman, N., and M. R. Stratton.** 1998. The genetics of breast cancer susceptibility. Annu. Rev. Genet. **32:**95–121.
38. **Rinaldo, C., P. Bazzicalupo, S. Ederle, M. Hilliard, and A. La Volpe.** 2002. Roles for *Caenorhabditis elegans rad-51* in meiosis and in resistance to ionizing radiation during development. Genetics **160:**471–479.
39. **Sharan, S. K., M. Morimatsu, U. Albrecht, D. S. Lim, E. Regel, C. Dinh, A. Sands, G. Eichele, P. Hasty, and A. Bradley.** 1997. Embryonic lethality and radiation hypersensitivity mediated by Rad51 in mice lacking Brca2. Nature **386:**804–810.
40. **Sharan, S. K., A. Pyle, V. Coppola, J. Babus, S. Swaminathan, J. Benedict, D. Swing, B. K. Martin, L. Tessarollo, J. P. Evans, J. A. Flaws, and M. A. Handel.** 2004. BRCA2 deficiency in mice leads to meiotic impairment and infertility. Development **131:**131–142.
41. **Siaud, N., E. Dray, I. Gy, E. Gerard, N. Takvorian, and M. P. Doutriaux.** 2004. Brca2 is involved in meiosis in *Arabidopsis thaliana* as suggested by its interaction with Dmc1. EMBO J. **23:**1392–1401.
42. **Suzuki, A., J. L. de la Pompa, R. Hakem, A. Elia, R. Yoshida, R. Mo, H. Nishina, T. Chuang, A. Wakeham, A. Itie, W. Koo, P. Billia, A. Ho, M. Fukumoto, C. C. Hui, and T. W. Mak.** 1997. Brca2 is required for embryonic cellular proliferation in the mouse. Genes Dev. **11:**1242–1252.
43. **Tsuzuki, T., Y. Fujii, K. Sakumi, Y. Tominaga, K. Nakao, M. Sekiguchi, A. Matsushiro, Y. Yoshimura, and T. Morita.** 1996. Targeted disruption of the Rad51 gene leads to lethality in embryonic mice. Proc. Natl. Acad. Sci. USA **93:**6236–6240.
44. **Tutt, A., D. Bertwistle, J. Valentine, A. Gabriel, S. Swift, G. Ross, C. Griffin, J. Thacker, and A. Ashworth.** 2001. Mutation in Brca2 stimulates error-prone homology-directed repair of DNA double-strand breaks occurring between repeated sequences. EMBO J. **20:**4704–4716.
45. **Venkitaraman, A. R.** 2002. Cancer susceptibility and the functions of BRCA1 and BRCA2. Cell **108:**171–182.
46. **Venkitaraman, A. R.** 2001. Functions of BRCA1 and BRCA2 in the biological response to DNA damage. J. Cell Sci. **114:**3591–3598.
47. **Walhout, A. J., G. F. Temple, M. A. Brasch, J. L. Hartley, M. A. Lorson, S. van den Heuvel, and M. Vidal.** 2000. GATEWAY recombinational cloning: application to the cloning of large numbers of open reading frames or ORFeomes. Methods Enzymol. **328:**575–592.
48. **West, S. C.** 2003. Molecular views of recombination proteins and their control. Nat. Rev. Mol. Cell. Biol. **4:**435–445.
49. **Wong, A. K., R. Pero, P. A. Ormonde, S. V. Tavtigian, and P. L. Bartel.** 1997. RAD51 interacts with the evolutionarily conserved BRC motifs in the human breast cancer susceptibility gene brca2. J. Biol. Chem. **272:**31941–31944.
50. **Yang, H., P. D. Jeffrey, J. Miller, E. Kinnucan, Y. Sun, N. H. Thoma, N. Zheng, P. L. Chen, W. H. Lee, and N. P. Pavletich.** 2002. BRCA2 function in DNA binding and recombination from a BRCA2-DSS1-ssDNA structure. Science **297:**1837–1848.
51. **Yu, V. P., M. Koehler, C. Steinlein, M. Schmid, L. A. Hanakahi, A. J. van Gool, S. C. West, and A. R. Venkitaraman.** 2000. Gross chromosomal rearrangements and genetic exchange between nonhomologous chromosomes following BRCA2 inactivation. Genes Dev. **14:**1400–1406.
52. **Yuan, S. S., S. Y. Lee, G. Chen, M. Song, G. E. Tomlinson, and E. Y. Lee.** 1999. BRCA2 is required for ionizing radiation-induced assembly of Rad51 complex in vivo. Cancer Res. **59:**3547–3551.
53. **Zickler, D., and N. Kleckner.** 1998. The leptotene-zygotene transition of meiosis. Annu. Rev. Genet. **32:**619–697.